Motor unit dysregulation following 15 days of unilateral lower limb immobilisation

Thomas B. Inns[1], Joseph J. Bass[1], Edward J.O. Hardy[1, 2], Daniel W. Stashuk[3], Philip J. Atherton[1], *Bethan E. Phillips[1], *Mathew Piasecki[1]

[1]Centre Of Metabolism, Ageing & Physiology, MRC-Versus Arthritis Centre for Musculoskeletal Ageing Research and NIHR Nottingham BRC, University of Nottingham, Derby, UK. [2]Department of Surgery and Anaesthetics, Royal Derby Hospital, Derby, UK. [3]Department of Systems Design Engineering, University of Waterloo, Ontario, Canada. (*co-senior authors).

Abstract

Disuse atrophy, caused by situations of unloading such as limb immobilisation, causes a rapid yet diverging reduction in skeletal muscle function compared to muscle mass. While mechanistic insight into the loss of mass is well studied, deterioration of muscle function with a focus towards the neural input to muscle remains underexplored. This study aimed to determine the role of motor unit adaptation in disuse-induced neuromuscular deficits. 10 young, healthy male volunteers underwent 15 days of unilateral lower limb immobilisation. Intramuscular EMG (iEMG) was recorded from the vastus lateralis during knee extensor contractions normalised to maximal voluntary contraction (MVC) pre and post disuse-induced loss of function. Muscle cross-sectional area was determined by ultrasound. Individual MUs were sampled and analysed for changes in discharge characteristics and MU potential (MUP) shape and structure. Vastus lateralis CSA was reduced by approximately 15% which was exceeded by a two-fold decrease of 31% in muscle strength in the immobilised limb, with no change to the non-immobilised. Parameters of MUP size were largely reduced, while neuromuscular junction (NMJ) transmission instability increased at several contraction levels and MU firing rate reduced. All adaptations were observed in the immobilised limb only. These findings highlight impaired neural input following immobilisation reflected by suppressed MU discharge rate and instability of transmission at the NMJ which may underpin the disproportionate reductions of strength relative to muscle size.

Introduction

Disuse atrophy is the loss of skeletal muscle mass and function associated with decreased external loading or complete immobilisation. It is common in clinical settings following joint trauma, nerve injury, or prescribed bed rest, and progresses rapidly with reductions of strength occurring after just 5 days (Wall *et al.*, 2014). As such, it has been widely applied as an experimental model to investigate underpinning mechanisms in scenarios of space flight, prolonged bed rest, spinal cord injury, and ageing (Castro *et al.*, 1999; Narici & De Boer, 2011; Puthucheary *et al.*, 2013). The trajectory of decline is not linear; five days of unilateral lower limb suspension lead to ~3 % reduction in quadricep cross-

sectional area (CSA) (Wall *et al.*, 2014) and eight weeks of bed rest reduced quadriceps CSA by ~14% (Mulder *et al.*, 2006).

The loss of muscle strength is commonly reported to exceed the loss of muscle size. Following 8 weeks of bedrest, quadriceps CSA declined by 14% compared to a 17% decline in strength (Mulder *et al.*, 2006), while only 10 days of bed rest was enough to elicit a ~6% reduction in CSA and a ~14% reduction in knee extensor maximal voluntary contraction (MVC) (Monti *et al.*, 2021). Furthermore, meta-analysis of bed rest studies with a combined 118 participants across various lengths found no relationship between length of bed rest and muscle size, whereas muscle power reduction and bed rest duration were strongly related (Di Girolamo *et al.*, 2021). Numerous data provide mechanistic insight to muscle *atrophy*, including decreased MPS, increased MPB, mitochondrial dysfunction, insulin resistance, and histochemical markers of fibre denervation (Phillips *et al.*, 2009; Rudrappa *et al.*, 2016; Monti *et al.*, 2021), yet mechanistic insight into loss of muscle *function* is less clear.

Successful activation of muscle relies upon coordinated input to the motoneuron pool and synaptic transmission across neuromuscular junctions (NMJs), and increases in muscle force are mediated by the recruitment and rate modulation of functioning motor units (MUs). Biopsies from the VL following 10 days of bed rest revealed structural disruption at the NMJ (Monti *et al.*, 2021) suggesting a contribution to decreased muscle activation and function. Furthermore, electromyography amplitude (EMG) following 14-day unilateral lower limb suspension (ULLS) decreased in the immobilised limb along with peak torque, while immobilised limb mass remained unchanged (Deschenes *et al.*, 2002), highlighting that reduced activation occurs in a limb specific manner with unloading. The extent of atrophy is also muscle dependent which has led to the descriptors of 'atrophy resistant' and 'atrophy susceptible' muscles (Bass *et al.*, 2021). A recent systematic review consolidated previous work to date (Campbell *et al.*, 2019), and of the 40 studies included, 20 immobilised the knee, preventing use of one of the most functionally relevant muscle groups, i.e., the quadriceps. Furthermore, just 20 studies carried out voluntary neuromuscular assessment using EMG, although all used surface EMG. While the breadth of measured parameters remains helpful, they reveal little of the adaptation of MU characteristics, particularly at the NMJ.

The purpose of the study was to quantify neuromuscular changes by studying individual MU features in the immobilised and non-immobilised limbs by utilising iEMG to sample individual MUs from the VL pre and post 15-days of immobilisation. We hypothesised that, coinciding with a reduction in muscle mass and strength, NMJ transmission instability and MU firing rate variability would increase in the immobilised leg, with no change to the non-immobilised.

Methods

Ethical approval

This study was approved by the local University Research Ethics Committee (ethics code: 103-1809) and conformed with the Declaration of Helsinki. It was also registered online at clinicaltrials.gov (NCT04199923). Participants were recruited locally from the University of Nottingham via advertisement posters. After providing written informed consent to participate in the study, participants were screened for eligibility.

Participants

Ten healthy, young male participants were recruited to take part in the study. Characteristics are provided in Table 1. Informed consent was provided before a screening visit. Once eligibility was confirmed, participants were invited to the laboratory for initial testing.

Muscle ultrasound

Vastus lateralis (VL) cross sectional area scans (CSA) were taken at the mid-belly of the muscle. This was located by measuring the length from the midline of the patella to the greater trochanter and taking the middle value of that line. Following this, a narrow ultrasound probe (LA523 probe and MyLab™50 scanner, Esaote, Genoa, Italy) was used to find the medial and proximal borders of the muscle where the aponeurosis of the VL intersected with the *vastus intermedius*. Three axial plane images were collected following this line from both legs and subsequently analysed using ImageJ (Laboratory of Optical and Communication, University of Wisconsin-Madison, WI, USA) to quantify CSA.

Unilateral lower limb power

Explosive unilateral lower limb power was assessed using the Nottingham Power Rig (University of Nottingham; Bassey & Short, 1990). For this procedure, the participant was seated on the purpose-built rig with their knee at 90° when the foot was placed on the plate. The seat is designed as such to isolate power production from the lower limb. Following a countdown, the participant was instructed to perform an explosive push. The power exerted as displayed digitally was recorded as the highest of three attempts.

Maximal voluntary isometric contraction

Participants were seated in a custom-built isometric dynamometer. The knee joint angle was fixed at 90° while the hip joint angle at 110°. The ankle was secured in place to a plate connected to a force transducer. Three moderate intensity warm-up contractions were carried out with visual feedback of their force trace on a screen in front of them. Using a waist belt to prevent hip lifting and isolating the

knee extensors, participants were verbally encouraged to perform an isometric knee extension at maximal capacity.

Vastus lateralis motor point identification

Using low intensity percutaneous electrical stimulation (400V, pulse width 50 µS, current ~10 mA; delivered via a Digitimer DS7A, Welwyn Garden City, UK), the surface of the VL was explored to find the point producing the greatest visible twitch with the lowest current, i.e., the motor point (Piasecki *et al.*, 2016*a*).

Force and electromyography recording

Surface electromyography was arranged in a bipolar configuration. The recording electrode was placed over the identified motor point and the reference electrode over the patellar tendon (disposable self-adhering Ag-AgCl electrodes; 95 mm^2; Ambu Neuroline, Baltorpbakken, Ballerup, Denmark). A ground electrode was placed just above the reference electrode on the patella (Ambu Neuroline Ground). EMG signals were digitised (CED Micro 1401; Cambridge Electronic Design, Cambridge, UK) and Spike2 (version 9.00a, CED) software was used to provide a real-time display of the signal on screen. Peak twitch force was calculated using percutaneous electrical stimulation (Digitimer, UK), and the maximal M-wave was measured with surface electromyography at the motor point. The stimulating pen was placed over the femoral nerve in the inguinal fold and stimulation intensity was increased until the M-wave amplitude displayed in Spike2 plateaued. The peak force generated corresponding to the maximal M-wave was recorded, and all force signals were recorded at 100 Hz.

Intramuscular electromyography procedure

A concentric needle electrode (Ambu Neuroline model 740 25-45/25, Ambu, UK) was inserted at the *vastus lateralis* motor point. The recorded iEMG signals were sampled at 50 kHz and bandpass filtered from 10 Hz to 10 kHz (1902 amplifier, CED). A real-time display was observed using Spike2 (CED) and data were stored offline for analysis. Once the needle was inserted, contractions were carried out at 10% and 25% of the participants MVC following a visual target line. Six contractions were recorded at each intensity, with the needle electrode position altered between each to sample a broader range of MUPs (Jones *et al.*, 2021). From the original position, the needle electrode was slightly withdrawn, and the bevel rotated 180° at each depth and positioned to maximise signal to noise ratio. These voluntary contractions were held for 12 s with a 10-20 s rest in between each contraction.

EMG analysis

Decomposition-based quantitative electromyography (DQEMG) software was used to process raw EMG data. This involved the detection of MUPs and extraction of MUP trains (MUPTs) from individual MUs generated during sustained iEMG signals recorded during voluntary contractions at set intensities. MUPTs were excluded if they contained MUPs from multiple MUs or fewer than 40 MUPs. MUP templates were visually inspected to ensure markers were placed correctly to start, end, positive and negative peaks of the waveforms. MUP area was defined as the integral of the absolute value of MUP values recorded between start and end markers multiplied by the sampling time interval in µV/ms (Piasecki *et al.*, 2021*b*). MUP amplitude was determined as the measurement from the maximal positive and negative peaks of the waveform (Guo *et al.*, 2022). MUP complexity, measured as the number of turns, defined as the number of significant slope direction changes within the duration of the MUP of a height >20 µV. A near fibre MUP (NF-MUP) was obtained from each MUP by estimating the slopes of each MUP (Piasecki *et al.*, 2021*b*) and NMJ transmission instability, measured as near-NF-MUP jiggle, was determined as the normalised means of median consecutive amplitude differences (Piasecki *et al.*, 2021*b*). MU firing rate (MU FR) was recorded as the rate of occurrence per second of MUPs within a MUPT in Hz, and MU FR variability was determined as the coefficient of variation of the inter-discharge interval.

Immobilisation procedure

For the 15 days of immobilisation, a unilateral lower-limb suspension (ULLS) model was used. The knee joint was fixed at 75 degrees flexion using a hinged leg brace (Knee Post op Cool, Össur, Iceland. Figure 1) and the knee joint was fixed using an air-boot (Rebound Air Walker, Össur). Crutches were provided and adjusted according to the height of the participant and training on their effective use was provided. This ensured that the immobilised leg was not able to bear any weight. Tamper tags were attached to the boot so that adherence was maintained and replaced if it was necessary for the boot and brace to be removed for testing purposes, while the brace and boot remained in place at all other times including sleeping and bathing.

Follow-up testing visit

Following 15 days of ULLS, participants were invited back to the laboratory for post-immobilisation testing. All procedures carried out in the initial testing visit as described above were repeated in both the immobilised and control legs, specifically ultrasound, MVC, surface and intramuscular electromyography. In addition to measuring iEMG at 25% contraction intensity of follow-up MVC (i.e., relative force), iEMG was carried out at 25% of baseline MVC to compare motor unit characteristics at absolute force values, referred to as baseline MVC and follow-up MVC.

Statistical analysis

Statistical analysis of MVC and ultrasound CSA was carried out using GraphPad Prism version 9.1.0 (GraphPad Software, CA, USA). These factors were assessed using repeated measures 2-way analysis of variance with Šidak's post-hoc analysis. Two within-subject factors were assessed: time (pre and post) and leg (immobilised and control). Multi-level mixed effect linear regression models were used to analyse motor unit parameters, with leg (immobilised and non-immobilised) and time (pre and post) as factors in StataSE (v16.0, StataCorp LLC, TX, USA). Where no leg x time interactions were present, separate models were performed to assess effects of time. For all tests, significance was assumed if $p<0.05$.

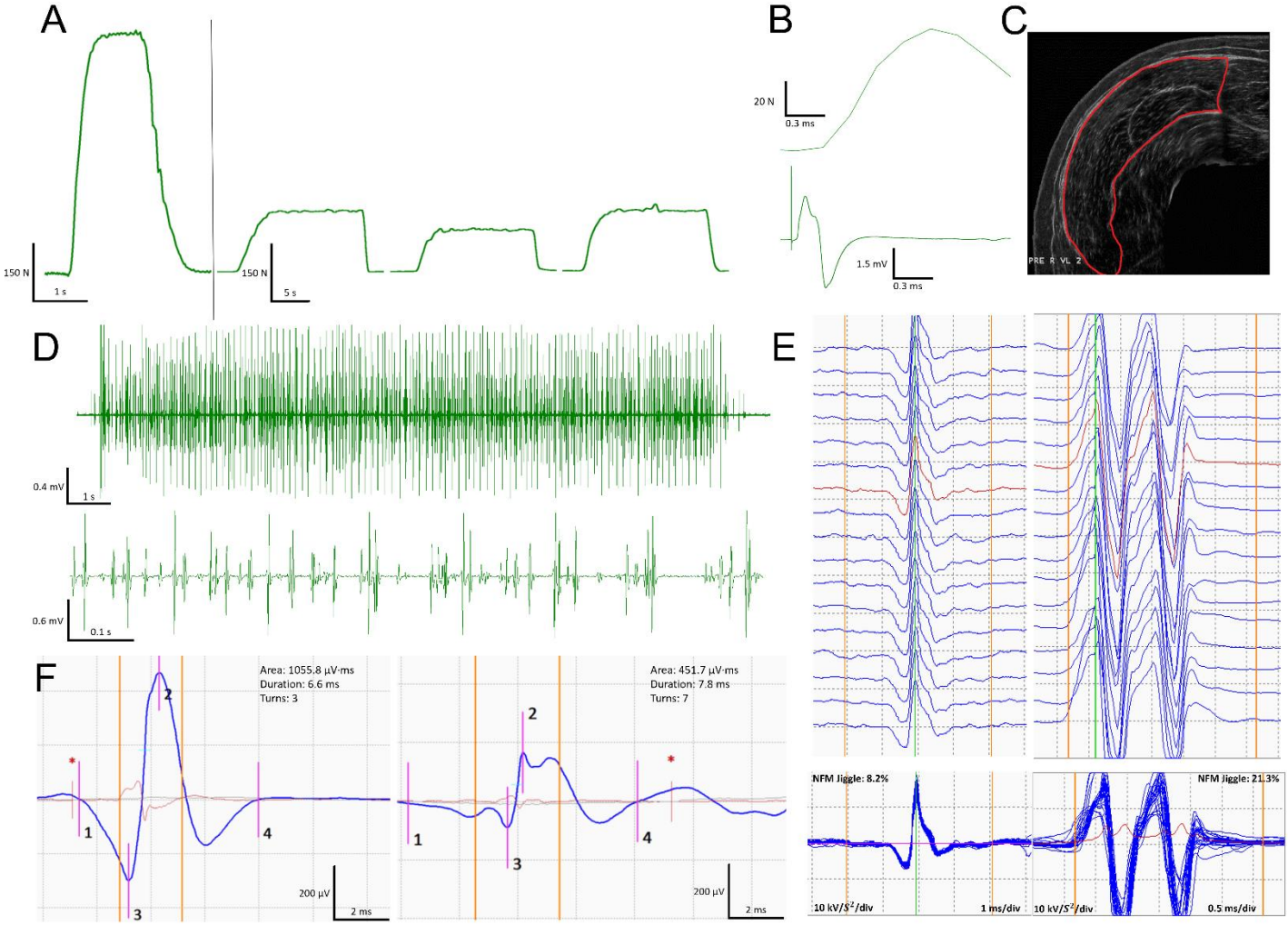

Figure 1: (A) *Knee extensor force traces (left to right) from a maximal voluntary isometric contraction (MVC), 25% of MVC contraction pre 15-day unilateral limb immobilisation, 25% contraction post-immobilisation relative to follow-up MVC, and 25% contraction post-immobilisation relative to baseline MVC.* ***(B)*** *Peak twitch force recording showing force trace (upper) and corresponding surface electromyography EMG recorded M-wave (lower) from a maximal stimulation of the femoral nerve.* ***(C)*** *An example ultrasound scan of the m. vastus lateralis used to calculate cross-sectional area.* ***(D)*** *Example intramuscular EMG (iEMG) trace recorded during a 12 second voluntary isometric contraction (upper) and magnified (lower) with visible motor unit potentials (MUP).* ***(E)*** *Example raster plots (upper) and corresponding shimmer plots (lower) from near-fibre MUPs (NF-MUP) before (left) and*

after (right) immobilisation recorded during active contractions. ***(F)*** *Example MUPs recorded before (left) and after (right) immobilisation. N; newtons, s; seconds, ms; milliseconds, V; volts, µV; microvolts, kV/s^2; kilovolts per second squared, µV·ms; microvolts per millisecond.*

Results

Participant Characteristics

Ten male participants took part in this study. Characteristics are shown in table 1.

Table 1: *Descriptive characteristics of participants showing mean and standard deviation (SD)*

N = 10	Mean (SD)
Age (years)	23.68 (3.36)
Height (cm)	181.56 (6.69)
Weight (kg)	79.37 (9.7)
BMI (kg/m^2)	24.02 (2.10)

Muscle Size and Function

There was a significant leg x time interaction in VL CSA ($p<0.001$), which decreased in the immobilised leg after 15 days (-15%, $p<0.001$) and remained unchanged in the control leg ($p=0.99$, Figure 2A). Similarly, there was a significant leg x time interaction of knee extensor MVC ($p<0.01$), which decreased in the immobilised leg (-31%, $p<0.001$) while no change was seen in the control leg ($p=0.498$, Figure 2B). Peak twitch force (n=7) showed no significant leg x time interaction ($p=0.058$). No change was seen in either the immobilised leg ($p=0.13$) or the control leg ($p=0.41$) following the immobilisation period (Figure 2C). Unilateral lower limb power output (n=9) presented a significant leg x time interaction ($p<0.05$) and following post-hoc analysis was reduced significantly in the immobilised limb (-26%, $p<0.05$) while remaining unchanged in the control leg ($p=0.94$, Figure 2D). Force steadiness (FS) at 10% MVC presented a significant leg x time interaction ($p=0.02$, figure 2E), reflected by a greater change in the immobilised limb (-14%, $p=0.077$) compared to the control (+4%, $p=0.278$). No interaction was present in FS at 25% MVC ($p=0.26$), with no changes seen following post-hoc analysis (immobilised: $p=0.999$, control: $p=0.221$, figure 2E).

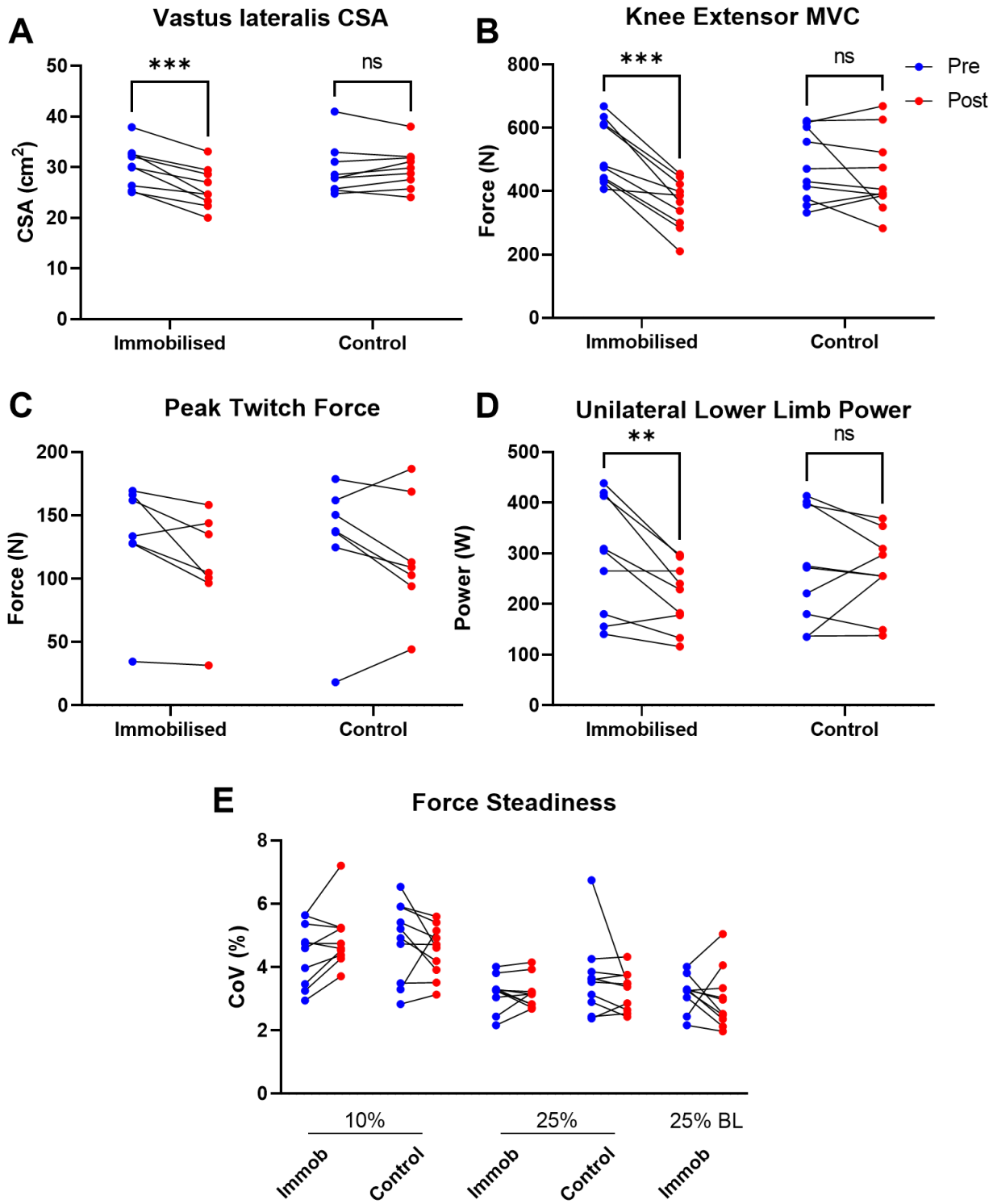

Figure 2: *All figures show data before and after 15-day unilateral lower limb suspension in the immobilised and control legs.* ***A:*** *Vastus lateralis cross-sectional area (cm^2) measured by ultrasound.* ***B:*** *Knee extensor maximal voluntary isometric contraction force (N).* ***C:*** *Peak twitch force (N, n=7) measured from maximal involuntary contraction elicited by femoral nerve stimulation.* ***D:*** *Unilateral lower limb power measured using the Nottingham Power Rig.* ***E:*** *Knee extensor force steadiness measured during contractions at 10 and 25% relative to both follow-up and baseline maximal voluntary isometric contraction. Coefficient of variation shown as average deviation from target line*

*(individual mean values shown pre to post in immobilised and control legs at each contraction intensity). For all parameters, analysis performed via repeated measures 2-way analysis of variance with Šidak's post-hoc analysis. ** = p<0.01, *** = p<0.001.*

Neuromuscular Parameters

Multi-level mixed effects linear regression models were used to examine individual motor unit adaptations recorded during 10% and 25% MVC contractions, before and after immobilisation in the VL of both legs. Contractions at 25% MVC were carried out relative to follow-up MVC as well as baseline MVC. Mean values for each parameter are shown in Figures 4 and 5. Due to no detectable MUPs from one participant post-immobilisation during 10% MVC contractions, for 10% MVC MUP parameter analysis and figures n=9. MUP area at 10% MVC presented no significant leg x time interaction (p=0.091, fig. 4A). Following post-hoc analysis, a reduction was seen in the immobilised leg (p<0.001) while no change was seen in the control leg (p=0.443). At 25% follow-up MVC, a significant interaction was seen (p<0.05, fig. 5A), with a reduction in the immobilised leg (p<0.001) but no change in the control (p=0.717). At 25% baseline MVC, significant reduction in MUP area (p<0.001) was present. For MUP amplitude at 10% MVC, there was no significant leg x time interaction (p=0.106, fig. 4B). In the immobilised leg a significant reduction was present (p<0.001) with no change in the control leg (p=0.283). At 25% follow-up MVC, amplitude presented a significant leg x time interaction (p<0.05, fig. 5B), with a reduction in the immobilised leg (p<0.01) but no change in the control (p=0.881). At 25% baseline MVC MUP amplitude was also significantly reduced (p<0.01).

MUP complexity, defined as the number of turns, presented no significant leg x time interaction at 10% MVC (p=0.66, fig. 4C), with post-hoc analysis showing an increase in the immobilised leg (p<0.05), but no change in the control (p=0.204). At 25% follow-up MVC, complexity had a significant leg x time interaction (p<0.05, fig. 5C). An increase was seen in the immobilised leg (p<0.01) but no change was seen in the control (p=0.6). At 25% baseline MVC MUP complexity did not change significantly (p=0.073). At 10% MVC, NMJ transmission instability showed no leg x time interaction (p=0.191, fig. 4D), with no change in either the immobilised (p=0.152) or control (p=0.759) legs. Similarly at 25% follow-up MVC, no leg x time interaction was seen (p=0.966, fig. 5D). However, a significant increase was seen in the immobilised leg (p<0.01) but no change in the control (p=0.164). At 25% baseline MVC, NMJ transmission instability was also increased (p<0.05).

Motor unit firing rate presented a significant leg x time interaction at 10% MVC (p<0.05, fig. 4E), with a reduction in the immobilised leg (p<0.001) but no change in the control (p=0.848). At 25% follow-up MVC, an interaction was also observed (p<0.001, fig. 5E), again showing a reduction in the immobilised leg (p<0.001) but no change in the control (p=0.563). At 25% baseline MVC, firing rate was also decreased (p<0.001). Finally, firing rate variability presented no leg x time interaction at 10% (p=0.07,

fig. 4F), with a reduction in the immobilised leg (p<0.01) and no change in the control (p=0.668). At 25% follow-up MVC, a significant interaction was seen (p<0.01, fig. 5F), with a reduction in the immobilised leg (p<0.001) and no change in the control (p=0.574). However, at 25% baseline MVC firing rate variability remained unchanged (p=0.193).

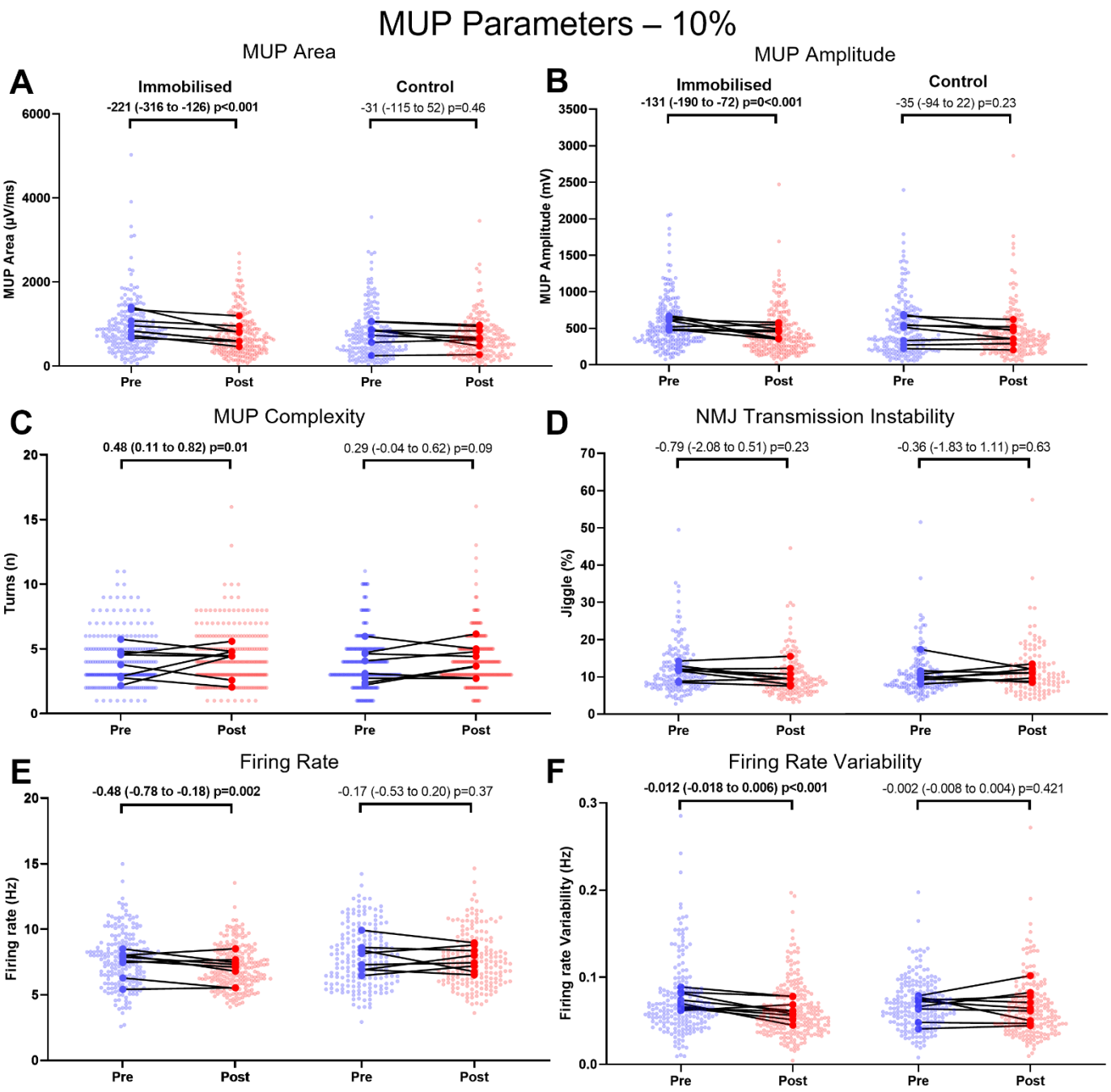

Figure 3: *Motor unit potential parameters and MU discharge characteristics of motor units sampled during contractions performed at 10% maximal voluntary force before and after 15-day unilateral leg immobilisation in both immobilised and control legs. Data show mean values and pooled MUs with comparison bars showing β coefficient and 95% CI from multi-level mixed effects models. N = 9.*

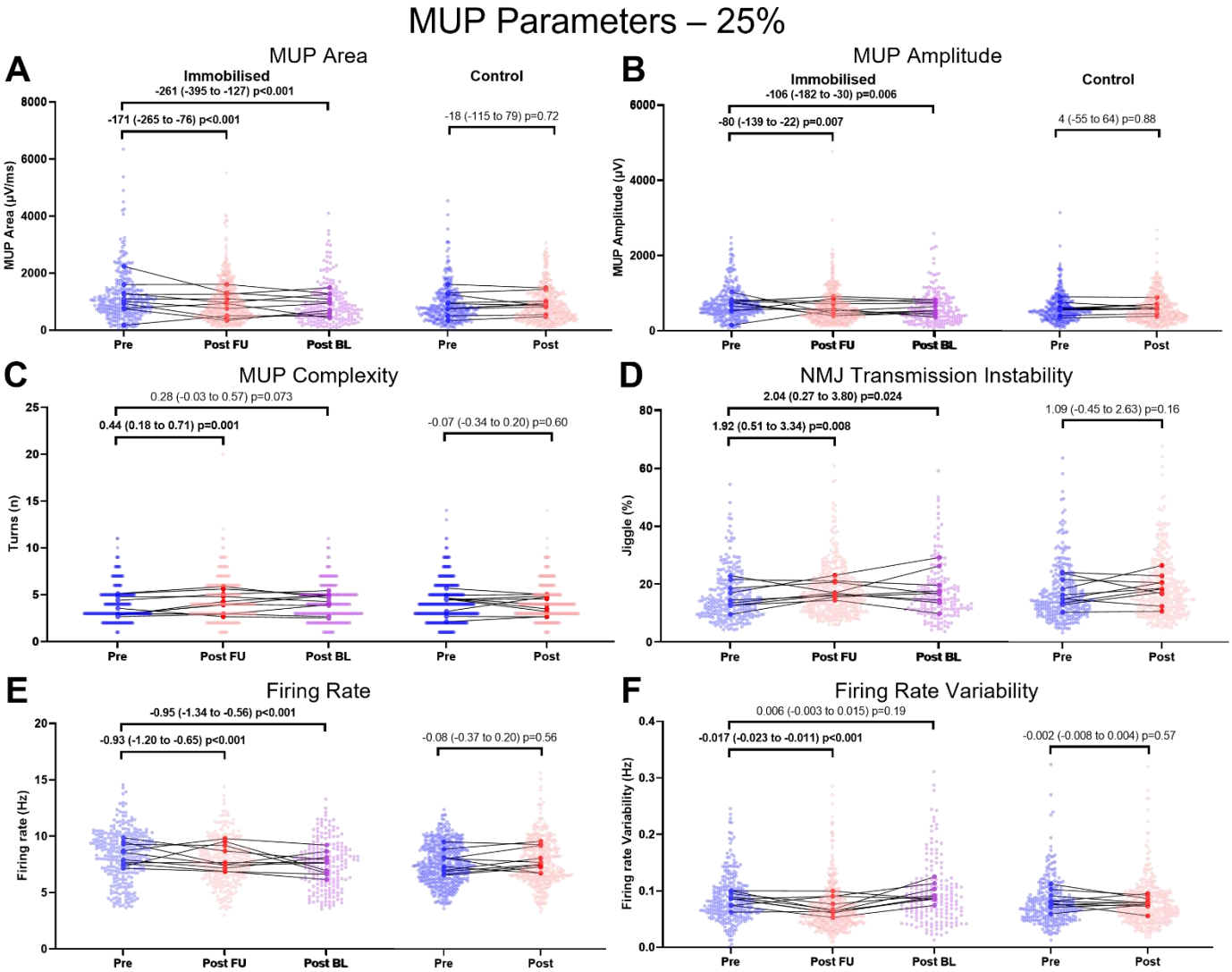

Figure 4: *Mean values of motor unit potential parameters and MU discharge characteristics of motor units sampled during contractions performed at 25% maximal voluntary force before and after 15-day unilateral leg immobilisation in both immobilised and control legs. Values in the immobilised leg post-immobilisation are relative to follow-up MVC (column 2) and relative to baseline MVC (column 3) due to reduced MVC following immobilisation. Data show mean values and pooled MUs with comparison bars showing β coefficient and 95% CI from multi-level mixed effects models.*

To investigate potential relationships between decline in strength and changes in neuromuscular parameters, correlations were performed between percentage change of MVC with firing rate and NMJ transmission instability 25% follow-up MVC (figure 6). A significant relationship was found between the reduction in MVC and the reduction in firing rate with simple linear regression (r2 = 0.62, p<0.01, figure 6A), while no correlation was observed between reduction in MVC and increase in NMJ transmission instability (r2 = 0.1, p=0.41, figure 6B).

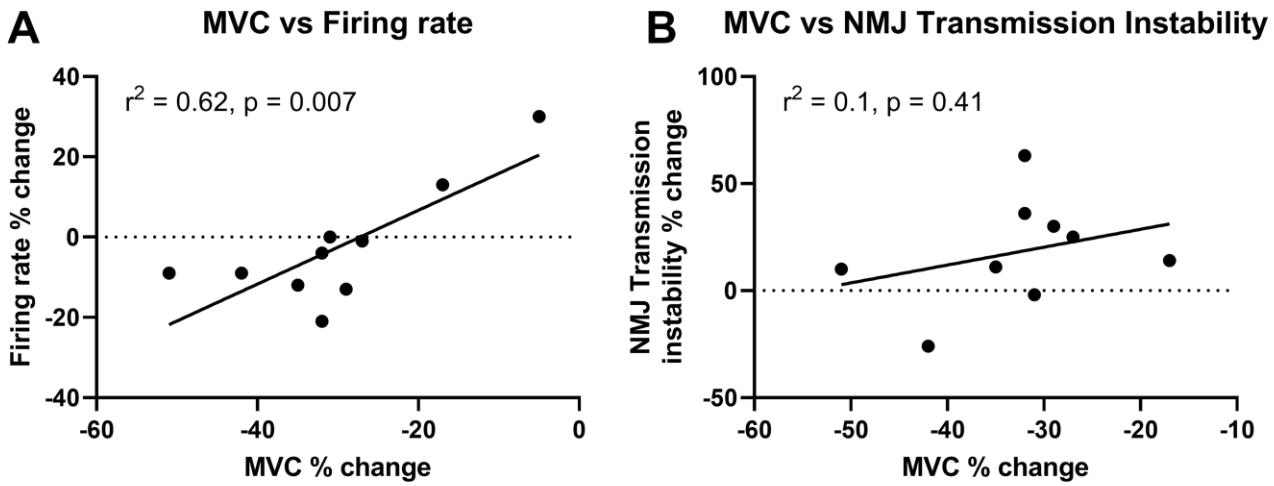

Figure 5: *Correlation and simple linear regression fit between reduction in maximal voluntary contraction (MVC) and motor unit firing rate (A) and neuromuscular junction (NMJ) transmission instability (B) recorded from contractions following immobilisation relative to the follow-up MVC at 25% MVC. N=9 for NMJ transmission instability due to a lack of high-quality motor units.*

Discussion

This study has characterised adaptations of individual VL MUs following 15 days of unilateral lower-limb immobilisation in immobilised and non-immobilised limbs. Our findings reveal a number of adaptations that are unique to the immobilised limb only, with the non-immobilised limb being largely unaffected. Muscle of the immobilised leg became smaller and weaker, and individual MUPs became smaller and more complex, had greater NMJ transmission instability, with reduced MU firing rate. Notably, these decrements were largely apparent when force levels were normalised to that achieved prior to immobilisation. This evidence highlights the impaired neural input to muscle as a large contributor to the observed reduction in muscle function.

The observed decline in muscle strength (-31%) in the immobilised limb exceeded the decline in muscle CSA (-15%), and this discordant finding supports several other studies employing a ULLS model; 14-day unilateral knee immobilisation with an 8% decrease in quadriceps CSA and a ~25% decline in isometric strength (Glover *et al.*, 2008), and ~8.5% decline in quadriceps CSA observed following 14 days of limb cast immobilisation, and a 31% decline in muscle strength (Wall *et al.*, 2014). Although measures of muscle CSA reveals little of fibre cross-bridge kinetics and calcium handling (Monti *et al.*, 2021), decrements of which also reduce force generating capacity, twitch force was also unaffected by immobilisation and although far from conclusive, these findings do support the inclusion of impaired neural input to muscle as a major contributing factor to functional losses. Neuromuscular control, as assessed by force steadiness normalised to MVC, was not affected by immobilisation at low or mid-range contraction intensities. This could suggest that sensorimotor capacity is protected following immobilisation, and although maximal force and power output are reduced, no significant change was seen with force steadiness normalised to baseline MVC. Unilateral power output was also only reduced in the immobilised limb. Bed rest studies have collectively shown a reduction in muscle performance of ~3% per day, although this reduction in bed rest was seen to stabilise between day 5 and day 14, suggesting a sharp initial reduction (Di Girolamo *et al.*, 2021) which may have also occurred in the present study. Furthermore, the control limb remained unaffected and does not support the concept of a negative cross-over effect on measures of neuromuscular function.

MUP size (area and amplitude) is reflective of the depolarisation of all fibres within a single MU, within the detection area of an indwelling electrode and is proportional to the size and number of fibres contributing to it. Area and amplitude were significantly decreased post-intervention at both 10 and 25% MVC contraction intensities in the immobilised leg only (figure 6A and 6B). While MUP size increase is commonly observed in reflecting MU remodelling and reinnervation of denervated muscle fibres (Jones *et al.*, 2022), the reduction observed here may indicate partial denervation of MU fibres as a result of disuse, or, it may reflect extensive fibre atrophy across MU fibres sampled at these

contraction levels. MUP size reduction has also been observed in dystrophinopathies (Zalewska *et al.*, 2013), where amplitude in the biceps brachii was significantly below reference values in patients with Duchene and Becker muscular dystrophies (Zalewska *et al.*, 2004). All markers of MUP size increase with increasing contraction level, reflecting the recruitment of additional, larger MUs (Guo *et al.*, 2022), and the decreases observed in the immobilised leg were apparent at 25% follow-up *and* baseline MVC. This finding highlights that reduction of force post-immobilisation cannot explain the decline in MUP size, and is more likely related to a reduction in muscle fibre size and/or partial denervation/reinnervation of fibres.

Similar to MUP size, MUP complexity, defined as the number of turns, was significantly greater in the immobilised leg only following the intervention, at both contraction intensities (figure 6C) which is indicative of a greater temporal electrophysiological dispersion between individual fibres of the same MU (Stålberg & Sonoo, 1994; Piasecki *et al.*, 2021*b*) as a result of an increased difference in conduction times along axonal branches and/or MU fibres. Increased MUP complexity has been observed in various myopathies which are suggestive of increased fibre diameter variability and also in neuropathies, expressing 75% greater turns than the control cohort, which is thought to be a product of the reinnervation and longer conduction times along axonal sprouts (Stewart *et al.*, 1989). This has been reinforced specifically in myopathic conditions, as data from primarily the biceps brachii along with recordings of the vastus lateralis and gastrocnemius showed an 82% increase in polyphasic MUPs (Uncini *et al.*, 1990). Although it has been suggested that complexity is less useful than other parameters to characterise myopathic and neuropathic disorders, it presents an interesting distinction between slow and rapid progressing disorders as well as those mild and severe (Zalewska *et al.*, 1998). While much less severe, the changes seen following immobilisation may also follow a common pathway linked to denervation and reinnervation. This may suggest that some reinnervation has occurred following immobilisation, or alternatively that selective reduction in muscle fibre diameter has taken place. Although needle insertions around the muscle motor point help to minimise the effects of variable muscle fibre conduction times and enable greater focus on axonal branch conduction variability, the specific motor endplate location remains an unknown *in vivo* and these effects cannot be completely excluded.

NMJ transmission instability, reported as NF MUP jiggle, was also significantly greater following the intervention in the immobilised leg only (figure 6D). NMJ structural stability was reported to decrease following 10-day bed rest, inferred following an increase in C-terminal agrin fragment (CAF) observed in serum at day 10 (Monti *et al.*, 2021). It is suggested that CAF presence may be indicative of a dysregulation at the NMJ, reducing myoelectrical transmission reliability and therefore contractile activity in the muscle. However, it is not clear if this evidence represents active NMJ transmission as

it is not directly measured during muscle contraction. Nevertheless, the *in vivo* methods applied here support the finding that disuse atrophy is accompanied by increased instability of transmission at the NMJ, possibly reflecting a partial denervation/reinnervation process. This process has been reported in healthy ageing (Hourigan *et al.*, 2015; Piasecki *et al.*, 2016*b*, 2021*a*) and diabetic neuropathy (Allen *et al.*, 2015) corresponding with larger MUPs. Abnormally high NF MUP jiggle values have also been reported in the tibialis anterior of patients with chronic inflammatory demyelinating polyneuropathy (Gilmore *et al.*, 2017) where an average of 90% increase compared to healthy controls was seen. This was also associated with increased MUP area and complexity, also attributed to an incomplete reinnervation process. NMJ transmission instability was also greater when contraction intensity was normalised to baseline MVC following immobilisation, indicating that NMJ dysregulation is prevalent through a wider pool of motor units responsible for a broader range of contraction force.

The reduced MU firing rate reported here is in agreement with well-established inverse relationship with muscle force and firing rate (De Luca & Hostage, 2010), since firing rate reduced following immobilisation during contractions based on 25% follow-up MVC, a lower absolute force value than pre-immobilisation. However, this suppression of firing rate was also apparent at contractions normalised to baseline strength and clearly highlights it as a contributor to functional decrements. Ionotropic synaptic inputs and neuromodulation control the excitability of motoneurons, the latter of which is largely mediated by the amplitude of persistent inward currents (PICs) which act to amplify synaptic input and are proportional to the level of localised monoamine release (Heckman *et al.*, 2008). Although difficult to quantify *in vivo*, it is possible monoamine levels decrease in response to reduced activity, yet it is unclear how this would influence the immobilised limb only. PIC amplitudes are also sensitive to inhibition (Hyngstrom *et al.*, 2007; Mesquita *et al.*, 2022), and recent RNAseq data highlight increased ligand-receptor interactions between muscle and dorsal root ganglion neurons following disuse, suggestive of an increased nociceptor sensitivity and susceptibility to pain (McFarland *et al.*, 2022). As such, it is possible increased inhibition occurred in the immobilised limb only and suppressed PIC amplitudes and MU firing rate. Reduction in firing rate variability at 10% MVC and 25% follow-up MVC may be viewed as a positive adaptation, however it more likely reflects the reduction in firing rate at lower absolute forces (Guo *et al.*, 2022) as it was not apparent when force was normalised to baseline MVC.

Additional analysis into factors potentially related to the reduction in force and changes in neuromuscular parameters found a significant positive correlation between the reduction in MVC and the reduction in firing rate following immobilisation in the immobilised leg recorded from contractions at 25% follow-up MVC. No significant relationship was found between reduction in MVC and increase

in NMJ transmission instability, which suggests that changes to firing rate, not NMJ transmission instability, are more influential in explaining loss of strength following immobilisation.

Since the average length of hospital stay in the United Kingdom as of 2018/19 was 4.5 days (Ewbank *et al.*, 2020), future work should focus on the impact of such a short time frame on the neuromuscular system. Understanding these changes will provide a basis on which improved rehabilitative systems can be put in place to counteract reduced muscle function.

Limitations

An inherent limitation to this method is that the contraction intensities at which motor units were sampled are of the low to mid-level and reveal nothing of adaptation to later recruited MUs. The current data are available in males only, and although we have highlighted similar differences across contractions in young males and females (Guo *et al.*, 2022), there are sex-based differences in MU firing rate at normalised contraction levels which may respond differently to this intervention.

Conclusion

These results support previous findings that unilateral short-term immobilisation leads to a decline in muscle strength unmatched by that of muscle size. Importantly, the current data highlight this disconnection is explained by central and peripheral adaptations to neural input to muscle, evidenced by suppressed MU firing rate and increased instability of transmission at the NMJ , occurring over as short a time period as 15 days and identifies further interventional targets in cases of muscle disuse.

References

Allen MD, Stashuk DW, Kimpinski K, Doherty TJ, Hourigan ML & Rice CL (2015). Increased neuromuscular transmission instability and motor unit remodelling with diabetic neuropathy as assessed using novel near fibre motor unit potential parameters. *Clin Neurophysiol* **126,** 794–802. DOI: 10.1016/j.clinph.2014.07.018.

Bass JJ, Hardy EJO, Inns TB, Wilkinson DJ, Piasecki M, Morris RH, Spicer A, Sale C, Smith K, Atherton PJ & Phillips BE (2021). Atrophy Resistant vs. Atrophy Susceptible Skeletal Muscles: "aRaS" as a Novel Experimental Paradigm to Study the Mechanisms of Human Disuse Atrophy. *Front Physiol* **12,** 1–11. DOI: 10.3389/fphys.2021.653060.

Bassey EJ & Short AH (1990). A new method for measuring power output in a single leg extension: feasibility, reliability and validity. *Eur J Appl Physiol Occup Physiol* **60,** 385–390. DOI: 10.1007/BF00713504.

Campbell M, Varley-Campbell J, Fulford J, Taylor B, Mileva KN & Bowtell JL (2019). Effect of Immobilisation on Neuromuscular Function In Vivo in Humans: A Systematic Review. *Sport Med* **49,** 931–950. DOI: 10.1007/s40279-019-01088-8.

Castro MJ, Apple DF, Rogers S & Dudley GA (1999). Influence of complete spinal cord injury on skeletal muscle mechanics within the first 6 months of injury. *Eur J Appl Physiol Occup Physiol* **81,** 128–131. DOI: 10.1007/PL00013785.

Deschenes MR, Giles JA, McCoy RW, Volek JS, Gomez AL & Kraemer WJ (2002). Neural factors account for strength decrements observed after short-term muscle unloading. *Am J Physiol - Regul Integr Comp Physiol* **282,** 578–583. DOI: 10.1152/ajpregu.00386.2001.

Ewbank L, Thomson J, Helen M & Anandaciva S (2020). NHS hospital bed numbers: past, present, future. *King's Fund*1–19. . Available at: https://www.kingsfund.org.uk/publications/nhs-hospital-bed-numbers [Accessed October 7, 2021].

Gilmore KJ, Allen MD, Doherty TJ, Kimpinski K & Rice CL (2017). Electrophysiological and neuromuscular stability of persons with chronic inflammatory demyelinating polyneuropathy. *Muscle and Nerve* **56,** 413–420. DOI: 10.1002/mus.25516.

Di Girolamo FG, Fiotti N, Milanović Z, Situlin R, Mearelli F, Vinci P, Šimunič B, Pišot R, Narici M & Biolo G (2021). The Aging Muscle in Experimental Bed Rest: A Systematic Review and Meta-Analysis. *Front Nutr* **8,** 1–13. DOI: 10.3389/fnut.2021.633987.

Glover EI, Phillips SM, Oates BR, Tang JE, Tarnopolsky MA, Selby A, Smith K & Rennie MJ (2008). Immobilization induces anabolic resistance in human myofibrillar protein synthesis with low and high dose amino acid infusion. *J Physiol* **586,** 6049–6061. DOI: 10.1113/jphysiol.2008.160333.

Guo Y, Jones EJ, Inns TB, Ely IA, Stashuk DW, Wilkinson DJ, Smith K, Piasecki J, Phillips BE, Atherton PJ & Piasecki M (2022). Neuromuscular recruitment strategies of the vastus lateralis according to sex. *Acta Physiol*1–14. DOI: 10.1111/apha.13803.

Heckman CJ, Johnson M, Mottram C & Schuster J (2008). Persistent inward currents in spinal motoneurons and their influence on human motoneuron firing patterns. *Neuroscientist* **14,** 264–275. DOI: 10.1177/1073858408314986.

Hourigan ML, McKinnon NB, Johnson M, Rice CL, Stashuk DW & Doherty TJ (2015). Increased motor unit potential shape variability across consecutive motor unit discharges in the tibialis anterior and vastus medialis muscles of healthy older subjects. *Clin Neurophysiol* **126,** 2381–2389. DOI: 10.1016/j.clinph.2015.02.002.

Hyngstrom AS, Johnson MD, Miller JF & Heckman CJ (2007). Intrinsic electrical properties of spinal motoneurons vary with joint angle. *Nat Neurosci* **10,** 363–369. DOI: 10.1038/nn1852.

Jones EJ, Chiou S, Atherton PJ, Phillips BE & Piasecki M (2022). Ageing and exercise-induced motor unit remodelling. *J Physiol* **600,** 1839–1849. DOI: 10.1113/jp281726.

Jones EJ, Piasecki J, Ireland A, Stashuk DW, Atherton PJ, Phillips BE, McPhee JS & Piasecki M (2021). Lifelong exercise is associated with more homogeneous motor unit potential features across deep and superficial areas of vastus lateralis. *GeroScience* **43,** 1555–1565. DOI: 10.1007/s11357-021-00356-8.

De Luca CJ & Hostage EC (2010). Relationship between firing rate and recruitment threshold of motoneurons in voluntary isometric contractions. *J Neurophysiol* **104,** 1034–1046. DOI: 10.1152/jn.01018.2009.

McFarland AJ, Ray PR, Bhai S, Levine BD & Price TJ (2022). RNA sequencing on muscle biopsy from a 5-week bed rest study reveals the effect of exercise and potential interactions with dorsal root ganglion neurons. *Physiol Rep* **10,** 1–14. DOI: 10.14814/phy2.15176.

Mesquita RNO, Taylor JL, Trajano GS, Škarabot J, Holobar A, Gonçalves BAM & Blazevich AJ (2022). Effects of reciprocal inhibition and whole-body relaxation on persistent inward currents estimated by two different methods. *J Physiol* **0,** 1–23. DOI: 10.1113/jp282765.

Monti E, Reggiani C, Franchi M V., Toniolo L, Sandri M, Armani A, Zampieri S, Giacomello E, Sarto F, Sirago G, Murgia M, Nogara L, Marcucci L, Ciciliot S, Šimunic B, Pišot R & Narici M V. (2021). Neuromuscular junction instability and altered intracellular calcium handling as early determinants of force loss during unloading in humans. *J Physiol* **599,** 3037–3061. DOI: 10.1113/JP281365.

Mulder ER, Stegeman DF, Gerrits KHL, Paalman MI, Rittweger J, Felsenberg D & de Haan A (2006). Strength, size and activation of knee extensors followed during 8 weeks of horizontal bed rest and the influence of a countermeasure. *Eur J Appl Physiol* **97,** 706–715. DOI: 10.1007/s00421-006-0241-6.

Narici M V. & De Boer MD (2011). Disuse of the musculo-skeletal system in space and on earth. *Eur J Appl Physiol* **111,** 403–420. DOI: 10.1007/s00421-010-1556-x.

Phillips SM, Glover EI & Rennie MJ (2009). Alterations of protein turnover underlying disuse atrophy in human skeletal muscle. *J Appl Physiol* **107,** 645–654. DOI: 10.1152/japplphysiol.00452.2009.

Piasecki J, Inns TB, Bass JJ, Scott R, Stashuk DW, Phillips BE, Atherton PJ & Piasecki M (2021*a*). Influence of sex on the age-related adaptations of neuromuscular function and motor unit properties in elite masters athletes. *J Physiol* **599,** 193–205. DOI: 10.1113/JP280679.

Piasecki M, Garnés-Camarena O & Stashuk DW (2021*b*). Near-fiber electromyography. *Clin Neurophysiol* **132,** 1089–1104. DOI: 10.1016/j.clinph.2021.02.008.

Piasecki M, Ireland A, Jones DA & McPhee JS (2016*a*). Age-dependent motor unit remodelling in human limb muscles. *Biogerontology* **17,** 485–496. DOI: 10.1007/s10522-015-9627-3.

Piasecki M, Ireland A, Stashuk D, Hamilton-Wright A, Jones DA & McPhee JS (2016*b*). Age-related neuromuscular changes affecting human vastus lateralis. *J Physiol* **594,** 4525–4536. DOI: 10.1113/JP271087.

Puthucheary ZA et al. (2013). Acute skeletal muscle wasting in critical illness. *JAMA - J Am Med Assoc* **310,** 1591–1600. DOI: 10.1001/jama.2013.278481.

Rudrappa SS, Wilkinson DJ, Greenhaff PL, Smith K, Idris I & Atherton PJ (2016). Human skeletal

muscle disuse atrophy: Effects on muscle protein synthesis, breakdown, and insulin resistance-A qualitative review. *Front Physiol* **7,** 1–10. DOI: 10.3389/fphys.2016.00361.

Stålberg E V. & Sonoo M (1994). Assessment of variability in the shape of the motor unit action potential, the "jiggle," at consecutive discharges. *Muscle Nerve* **17,** 1135–1144. DOI: 10.1002/mus.880171003.

Stewart CR, Nandedkar SD, Massey JM, Gilchrist JM, Barkhaus PE & Sanders DB (1989). Evaluation of an automatic method of measuring features of motor unit action potentials. *Muscle Nerve* **12,** 142–148. DOI: 10.1002/mus.880120209.

Uncini A, Lange DJ, Lovelace RE, Solomon M & Hays AP (1990). Long-duration polyphasic motor unit potentials in myopathies: A quantitative study with pathological correlation. *Muscle Nerve* **13,** 263–267. DOI: 10.1002/mus.880130315.

Wall BT, Dirks ML, Snijders T, Senden JMG, Dolmans J & Van Loon LJC (2014). Substantial skeletal muscle loss occurs during only 5 days of disuse. *Acta Physiol* **210,** 600–611. DOI: 10.1111/apha.12190.

Zalewska E, Hausmanowa-Petrusewicz I & Stålberg E (2004). Modeling studies on irregular motor unit potentials. *Clin Neurophysiol* **115,** 543–556. DOI: 10.1016/j.clinph.2003.10.031.

Zalewska E, Rowińska-Marcińska K & Hausmanowa-Petrusewicz I (1998). Shape irregularity of motor unit potentials in some neuromuscular disorders. *Muscle and Nerve* **21,** 1181–1187. DOI: 10.1002/(SICI)1097-4598(199809)21:9<1181::AID-MUS9>3.0.CO;2-3.

Zalewska E, Szmidt-Salkowska E, Rowinska-Marcinska K, Kaminska A & Hausmanowa-Petrusewicz I (2013). Motor unit potentials with satellites in dystrophinopathies. *J Electromyogr Kinesiol* **23,** 580–586. DOI: 10.1016/j.jelekin.2012.11.002.